Structural Engineering and Mechanics, *Vol. 72, No. 1 (2019) 19-30*
DOI: https://doi.org/10.12989/sem.2019.72.1.019

Experimental and analytical investigation of the shear behavior of strain hardening cementitious composites

Antroula V. Georgiou*[1] and Stavroula J. Pantazopoulou[2a]

[1]*Department of Civil and Environmental Engineering, University of Cyprus, #1 University Ave., P.O. Box 20537, 1678 Nicosia, Cyprus*
[2]*Dept. Civil Engrg., Lassonde Fac. of Engrg., York Univ., Toronto, ON M3J 1P3, Canada*

(Received October 8, 2018, Revised April 23, 2019, Accepted May 17, 2019)

Abstract. The mechanical behavior of Fiber Reinforced Cementitious Composites (FRCC) under direct shear is studied through experiment and analytical simulation. The cementitious composite considered contains 55% replacement of cement with fly ash and 2% (volume ratio) of short discontinuous synthetic fibers (in the form of mass reinforcement, comprising PVA - Polyvinyl Alcohol fibers). This class of cementitious materials exhibits ductility under tension with the formation of multiple fine cracks and significant delay of crack stabilization (i.e., localization of cracking at a single location). One of the behavioral parameters that concern structural design is the shear strength of this new type of fiber reinforced composites. This aspect was studied in the present work with the use of Push-off tests. The shear strength is then compared to the materials' tensile and splitting strength values.

Keywords: shear; strain hardening cementitious composites; discontinuous fibers; push-off

1. Introduction

Sustainable design of structures necessarily leads to reduction of the exploitation of natural materials sourced from the earth (aggregates, cement) and their replacement with recycled aggregates or industrial byproducts, such as high amounts of fly ash (>50%). Another very effective aspect of sustainability is enhancement of durability of structures through control of cracking and crack propagation by means of dispersed fibers in the cementitious matrix, thereby extending the dependable service life of the structure (Georgiou and Pantazopoulou 2016c). In the same direction of durability enhancement fine additives such as Fly Ash in high amounts serves to achieve a dense compaction, acting both as a pozzolan and as a filler. Research in the past few decades led to the development of a new generation of cementitious composites with markedly improved tensile strength and strain resilience, distributed fine cracking prior to crack stabilization. This technology was effected by proper design of the cementitious matrix and through optimization of the fiber surface properties so as to encourage gradual slip rather than rupture at crack locations.

The macroscopic effect on the tensile stress-strain properties of the cementitious material creates a new opportunity in design, where the significant amounts of detailing reinforcement which was considered essential for sustained shear and bond resistance may now be partly mitigated by the sustained resistance of concrete in tension up to large levels of average tensile strain. From among the many types of fibers commonly used today in engineered cementitious composites, a commonly used option is Polyvinyl-Alcohol (PVA) fibers, on account of their strongly hydrophilic surface; if embedded in concrete they tend to create strong chemical bonds with the surrounding matrix, which increase further with age (Li *et al*. 2003, Georgiou and Pantazopoulou 2016b). However, the strength of the interfacial bonds is one aspect that can be moderated to a desirable level through proper surfactants; by attenuating the strength of the interfacial bonds on the fiber surface it is possible to control fiber pullout, so as to eliminate the tendency for crack localization with increasing age (Georgiou and Pantazopoulou 2016b), thereby ensuring fine distributed cracking in Fiber Reinforced Cementitious Composites (FRCC - this term was coined by Naaman and Reinhardt 2006).

The emerging Strain Hardening Cementitious Composites (SHCC) is a special category of FRCCs, which not only present toughness to large tensile deformation, but also strain hardening properties. The entire class of these materials has a matrix that lacks any coarse aggregates, containing only fine high quality sand with maximum particle size less than 300μm. Additionally for improving the sustainability of these composites the matrix has great amounts of cement replacement to fly ash, even in the order of 60%. This special class of cement-based composites has shown enhanced flexural performance whereas the enhanced tensile strain hardening behavior mitigates susceptibility of shear resistance to cracking. The materials used also show self compacting properties of the matrix. Zarrin and Khoshnoud (2016) have revealed through tests that Self-Compacting Concrete with steer fibers improves the mechanical properties and durability of hardened concrete as well as its post-cracking behavior, therefore the SHCC adopted in this investigation had also the ability of

*Corresponding author, Ph.D.
E-mail: ageorg44@ucy.ac.cy
[a] Professor

ISSN: 1225-4568 (Print), 1598-6217 (Online)

self-compactness. Tests conducted on structural members reveal that this beneficial effect at the material level, is bestowed also on the overall structural performance effectively governing the mechanics of complete structural members (Georgiou and Pantazopoulou, 2017, Toshiyuki *et al*. 2013).

To anticipate the behavior of these materials in shear, it is useful to refer to the relevant mechanisms of resistance in conventional concrete. These include, a) the dowel action of reinforcement intersecting the cracks, b) the friction between crack faces and aggregate interlock, c) the residual diagonal strength of cracked concrete. Elimination of coarse aggregate means that there is no aggregate interlock – which, in conventional concrete is considered an essential source of post-cracking shear resistance. Instead, in SHCC the postcracking shear strength and resilience is – to a large extent – owing to the use of the short fibers. Other mechanisms such as dowel action and compressive strength of cracked concrete also prevail in the SHCC members, however, there is a need to better understand these strength components and to quantify the shear resistance of steel reinforced SHCC members for the benefit of practical design. To quantify the behavior of SHCC in shear, either beam tests or direct shear tests have been conducted in relevant experimental studies; beam tests were studied before, where it was shown that concrete shear contribution owing to the fibers may be set equal to the flexural modulus of the material developed, and this was related to the volumetric ratio and the aspect ratio of the fibers, as well as the tensile properties of plain concrete (Georgiou and Pantazopoulou 2017). Investigation of the contribution of SHCC in shear was performed also for the retrofit of reinforced concrete buildings by means of enhancing their ductility using infilled SHCC walls (Chang-Geun *et al*., 2008) proposing a shear model based on the Modified Compression Field Theory to model the behavior of the in-filled SHCC panels.

In the present study, push-off specimens are used to explore and explain the role of the fibers in the mechanics of shear of SHCC members. Note that in the absence of coarse aggregates, aggregate interlock is eliminated as a possible mechanism of shear resistance. Mass reinforcement in the form of fibers affects the overall shear behavior and interacts with the steel stirrups when these exist. Clearly, the mechanics of shear transfer in this type of composite studied are very different from what is currently known for normal concrete. Nevertheless, studying the behavior in shear is considered a priority and prerequisite for improving the implementation of the composites in structural applications. The shear strength of reinforced concrete beams with longitudinal bars in the presence of reinforcing steel fibers with and without transverse stirrups has been studied by Qissab and Salman (2018) and Campione *et al*. (2006) respectively who derived semi-empirical analytical expressions to account for the shear contribution of fibers based on the material's characteristics. These expressions are well suited for steel fiber reinforced composites that present a strain softening behaviour in tension, while the performance of a strain hardening composite as presented in the current research, is still under investigation.

The shear behavior in this research was studied using the so-called direct shear tests; in fact this test type may elucidate the basic shear transfer mechanics, whereas beams are more relevant to member behavior in flexure-shear. Note that past studies on conventional FRC in shear indicate that fibers generally improve shear strength and ductility of concrete and that they may partially be used to reduce the amounts of stirrups (Parra-Montesinos 2005). Kang *et al*. (2017) and Zhao *et al*. (2017) performed preliminary studies on the shear behavior of SHCC with push off tests and and composites that included ground granulated blast furnace slag, comparing it with normal strength concrete concluding that shear strength and strain increases due to the presence of fibers. The push-off tests conducted herein were intended to experimentally quantify the shear strength in relation to the tensile properties of the SHCC material studied, in light of the fact that the sliding plane of the direct shear specimen experiences a state of pure shear which is equivalent to the simple diagonal tension that occurs in the web of beams under load.

2. Experimental program

Apart from the tests conducted to study the shear behavior of SHCC, auxiliary tests were also carried on a series of specimens in order to determine the uniaxial material stress-strain curves in direct and indirect tension as well as direct compression. In each case, three identical specimens were tested for each type of test and mix design. Specimens were tested at the age of 100 days, in order to acquire the long term mechanical properties of the composites, since the pozzolanic activity of fly ash along with the coating of the fibers affect gradually the interfacial bond properties between the fibers and the matrix and therefore impact the multiple cracking phenomenon, thereby altering the material's strain capacity (Wang and Li, 2006). Uniaxial compression tests were performed on cylinder specimens 100 mm in diameter and 200 mm in height; the aspect ratio of 2 was used in order to eliminate the local end effects, under displacement control, at a loading rate of 1.5 μm/s (Fig. 1 (a)). For the determination of uniaxial tensile strength both direct tension (dog-bone type) tests and split cylinder tests were conducted. Direct tension tests (Fig. 1 (b)) were performed at a displacement control rate of 2.5 μm/sec with a gauge length of 100 mm. Deformations were recorded with two LVDTs mounted on opposite sides of the specimens. The split cylinders had a diameter of 100mm and a height of 100 mm. The splitting tests (Fig. 1 (c)) were conducted under displacement control at a displacement rate of 0.5 mm/min.

The direct shear behavior of the mixes was investigated with the use of uncracked push-off specimens (Fig. 1 (d)). The specimens had dimensions of 250x500x100 mm as shown in Fig. 2 (a), with a shear plane area of 100x200=20000 mm^2 as proposed from previous research (Valle and Buyukozturk 1993, Buyukozturk *et al*. 1990). Two parameters were investigated:

a) the mix design – i.e., with or without fibers: to this end, two mixes, denoted as HVFA and SHCC were

(a) Uniaxial compression test (b) Uniaxial Tension (c) Split Cylinder Test (d) Push-off test

Fig. 1 Testing Apparatus

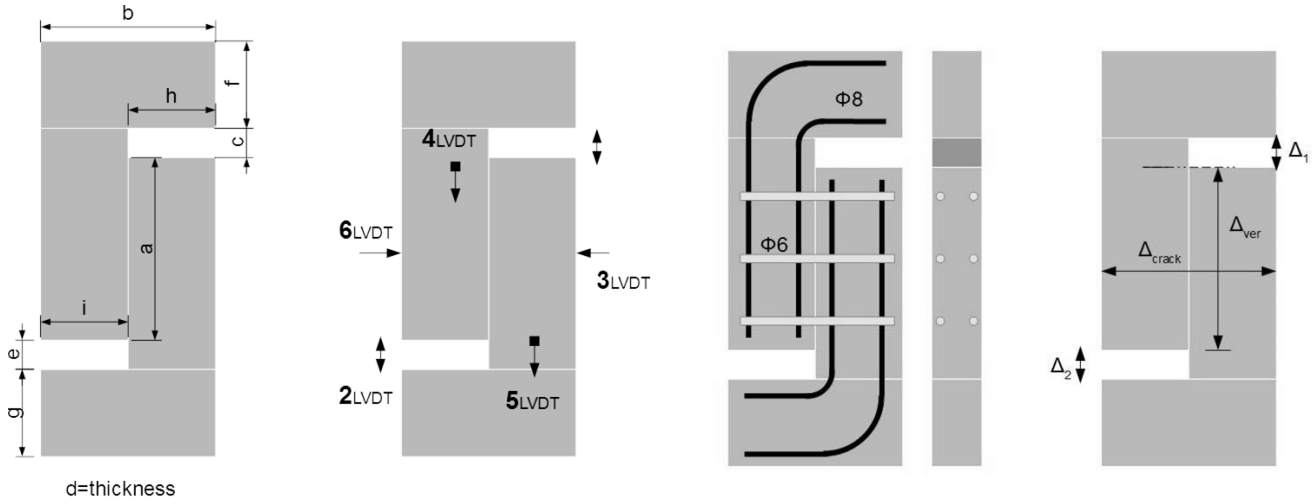

(a) specimen geometry (b) deformation measurement system (c) reinforcement setup (d) definition of deformation for graphical representation

Fig. 2 Push off specimen

Table 1 Specimen Denomination

Push-off specimen identification	Mix design	Stirrups
HVFA	HVFA	-
HVFA-S	HVFA	6Φ6
SHCC	SHCC	-
SHCC-S	SHCC	6Φ6

considered. (Specifically, HVFA was the basic mix used in the study, with a high volume fly ash used as cement replacement whereas SHCC was the same mix but with the addition of PVA fibers).

b) the availability of steel stirrups crossing the shear plane was also a study variable. Specimens containing stirrups had the configuration shown in Fig. 2 (c).

Three identical specimens were tested for each type of test and mix design. The specimen's classification and identifying names are outlined in Table 1. For the push-off specimens LVDTs were used to measure displacements at various positions (Fig. 2 (b)). Note that the horizontal relative displacement of the vertical specimen boundaries is actually an estimate of the crack width developing along the shear plane. The test was performed under displacement control at a speed of 7 μm/sec for the specimens without stirrups and 15 μm/sec for the specimens with stirrups. Table 2 gives indicative values of the geometrical dimensions of the push off specimens.

Table 2 Indicative values of the geometrical dimensions of the push off specimens (in mm)

a	**b**	**c**	**d**	**e**	**f**	**g**	**h**	**i**
200	250	30	100	30	125	125	125	125

3. Materials

3.1 Fiber Reinforced Composites

The mix designs used for (a) the plain mix with high volume of fly ash (HVFA) and (b) the same mix with the fibers (SHCC) are listed in Table 3. Portland Composite Cement 42.5 R and silica sand (>95% Si) with a maximum grain size of 300 μm were used. The silica sand had spherical crystal quartz particles showing a very narrow grain size distribution and a high SiO_2 content (percentage of silica oxide is in the order of 98.6%, Mohs Hardness is 7,

Table 3 Mixture proportions (*per weight, $^{+}$ per volume)

MIX	Cem.*	FA*	Sand*	Water*	S/P*	Fibers^{+}	Coating*
HVFA	1.00	1.20	0.80	0.55	0.012	-	-
SHCC	1.00	1.20	0.80	0.60	0.017	2%	6.6%

Table 4 Steel reinforcement characteristic points from tensile tests

Steel Reinf.	ε_{sy}	ε_{syy}	ε_{su}	f_{sy} (MPa)	f_{syy} (MPa)	f_{su} (MPa)
φ6	0.0026	0.026	0.2	312	320	376

raw density is 2.65 gr/cm^3, bulk density is 1.35 gr/cm^3). Type F fly ash was used as cement replacement. This type of fly ash has pozzolanic properties that enhance the performance of concrete (complies fully with ASTM C618 (2008) and EN 206 (2013)). This fly-ash contains extremely fine (0.45 μm) latently reactive silicon dioxide. Class F FA is indicated to be used as cement replacement at fractions ranging from 20-30% of the mass of cementitious material but in the present investigation the amount of FA used was 120% by weight of the amount of cement (that is, one part of binder in the final mixture comprised 45% cement and 55% fly-ash). PVA fibers (12mm long, 39 μm diameter (dtex15)) were used at 2% volume fraction, with 1300 kg/m^3 density, nominal tensile strength of 1600 MPa and 40 GPa Young's Modulus. The fibers were coated with a pertinent surfactant at a weight ratio of 6.6% of the weight of fibers as per (Georgiou and Pantazopoulou, 2016a). PVA fibers have free hydroxyl groups in their molecular chain promoting chemical bonding with the surrounding cementitious matrix. The strong interfacial bonds lead to fiber rupture rather than pull-out, resulting in higher tensile strength but lower ductility. Chemical treatment of fibers with surfactants decreases the interfacial bonding. Past studies have shown that coating the PVA fibers increases their dispersion whereas the final ductility of composites is controlled by the bond properties at the fiber - matrix interface.

3.2 Steel Bars

Uniaxial tension tests were performed on samples of the steel reinforcement used in constructing the specimens. The reinforcing steel was 6mm diameter smooth wire with 300 MPa yield strength and 200 GPa modulus of elasticity. The smooth bars used for stirrup reinforcement were hook-anchored into the member core. Table 4 lists values for milestone points in the stress-strain diagram of the reinforcing materials.

3.3 Mixing and Casting of Specimens

The mixing sequence that was used took into consideration the special character of the materials and their impact on the rheological properties of the mix. The first step was mixing of all the dry materials –cement, fly ash and sand; this was performed within the mixer for at least 30 minutes. The water was mixed separately with the super-plasticizer prior to adding it to the cement in order to ensure full development of the chemical reaction between the super-plasticizer and the cement. Then 90% of the liquid part was added in the dry material mix. Once the dry components were adequately mixed with the liquid part, fibers were slowly added in small amounts and the rest of the liquid part was added in the end. Care was taken in order to ensure that fibers would not lump-up. Once the mixing procedure was completed the specimens were cast into molds.

Specimen fabrication was done according with the following steps: a) Steel cages were prepared for the specimens where necessary (no reinforcement was necessary for the configuration of specimens comprising SHCC and no stirrups). Vertical reinforcement was found to be necessary for the configuration of specimens without fibers and without stirrups because when tested without, failure occurred in premature modes other than sliding along the shear plane (e.g. flexural cracking of the top and bottom levers between the notches and the loading plattens). Vertical reinforcement was tied using closed stirrups of 6mm diameter, b) Reinforcement was placed in the molds with the appropriate spacing. In order to create the notches needed to form the shear plane, polyurethane prisms were placed in the molds and firmly secured in order not to move during casting, c) Casting of the specimens was performed without the use of any vibration since both of the mixes were self-compacting (filling ability was measured by the slump flow method as per (EN 12350-8:2010, 2010) giving values of 925mm for the HVFA and 705mm for the SHCC), d) After the specimens were casted they were left in the molds for 24 hours, covered with plastic sheets, e) Specimens were demolded and placed in water if not containing any reinforcement, while the ones that had reinforcement were wrapped in wet burlap and covered by plastic sheet until the testing date. For the push-off specimens 6 LVDTs were used, as shown in Fig. 2 (b) to measure displacements at various positions. LVDTs #3 and #6 were used to measure horizontal displacement of the specimen, which is actually the vertical crack width defined normal to the shear plane.

4. Test Results

4.1 Material characterization in tension and compression

In the case of the HVFA mix (i.e., plain matrix) the three samples that were cast for uniaxial tension, cracked during de-molding. The SHCC mix on the other hand demonstrated strain hardening response in uniaxial tension: during the phase of multiple crack formation, stress capacity of the cross section increased (Fig. 3 (d)). Details of the experimental setup for the uniaxial tensile test are given elsewhere (Georgiou and Pantazopoulou, 2016c). Past a notional yield point multiple cracks formed whereas fibers were bridging the cracks transferring load. Formation of cracks saturated the full length till the occurrence of crack localization and failure. The fracture energy G_f, which is defined as the area under the stress- crack opening curve in

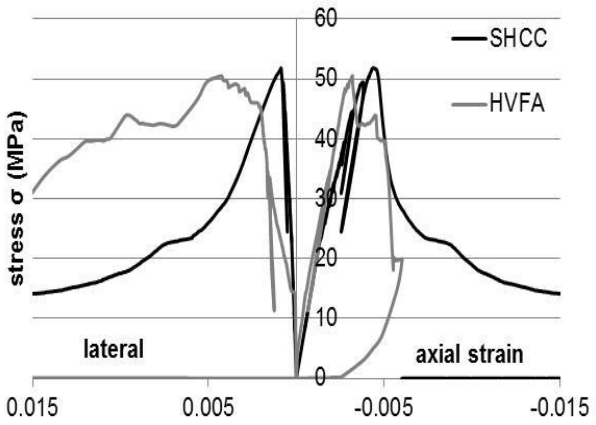

(a) Stress - axial/lateral strain diagrams under compression of HVFA and SHCC mixes

(b) failure cracks for HVFA

(c) failure cracks for SHCC

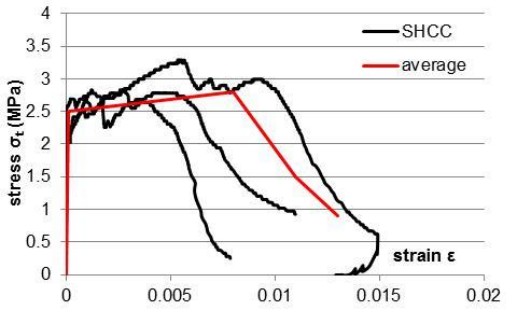

(d) stress-strain curve of SHCC under uniaxial tension

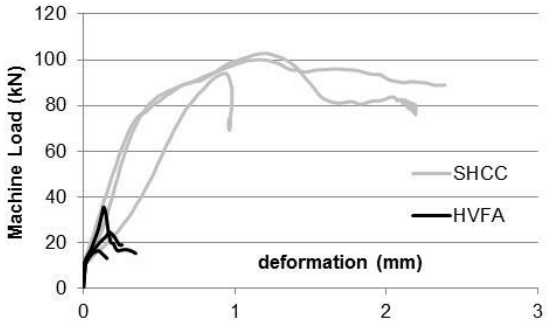

(e) split cylinder test load-lateral deformation

Fig. 3 Material characterization

the strain softening branch past the ultimate stress was estimated as G_f=1065 N/m for the SHCC - a value much greater than the expected one for ordinary strength cement mortars and concretes which is in the order of 50 N/m and 130 N/m respectively (Archontas and Pantazopoulou, 2015). To acquire the tensile strength of the HVFA composite splitting test was employed based on the ASTM Standard specifications (ASTM C496, 2006) as $f_{split}=2P/(\pi l \cdot d)$. The average Load P at failure of the three HVFA specimens was P=25.46 kN (Fig. 3 (e)), (the average splitting tensile strength was f_{split}=1.62 MPa); but the splitting tensile strength of the SHCC mix was f_{split}=6.4 MPa while its average tensile strength under uniaxial tension was 2.65 MPa.

Figure 3 (a) compares the stress - axial strain - lateral strain diagrams obtained from compression tests conducted on one of the specimens with the use of fibers (SHCC) and of one of the tested specimens of the same matrix without the fibers (HVFA). The average compressive strength of the latter reaches 50.4MPa, but with the addition of fibers the average strength decreases to 49.0MPa. An increase by more than 30% occurred in the axial deformation capacity at peak load as compared to the corresponding values for plain mixes in the case of the matrix with the fibers (average strain at peak stress from -0.0032 for the HVFA to -0.00459 for the SHCC), as well as a more stable descending branch. Based on the uniaxial compression experimental results of fiber reinforced cementitious composites as shown in Fig. 2 multiple cracking is visible all around the specimen, but there is no evidence of disintegration or collapse of the cylindrical concrete block even after a 60% drop of the postpeak resistance under compression. In the case of the plain matrix (HVFA), a precipitous decay occurred past the peak point accompanied with complete disintegration of the specimen. Therefore the use of fibers altered the mode of failure. Past research has illustrated that lateral deformation is responsible for the rate of descend of the post peak branch. Thus, the fibers were mobilized in the lateral direction bridging the cracks, transferring load and limiting the lateral expansion of the cylinder under compression, acting as an effective internal transverse confinement (Georgiou and Pantazopoulou, 2017). This is evidenced by the restricted growth of post-peak lateral strain of the mix with fibers as compared to the plain concrete specimens. The intensity of the internal confinement was found to be directly related to the materials' strength under splitting (Georgiou and Pantazopoulou 2017).

4.2 Behaviour of specimens under push-off

Failure modes of all tested specimens are depicted in Figure 4 (c). Specimens HVFA without steel stirrups failed in a brittle mode as soon as the shear plane reached peak shear strength. Figure 5 shows the sequence of crack formation of one of the specimens without fibers but with steel reinforcement (HVFA-S). In the beginning a shear crack was created along the shear plane. After cracking of

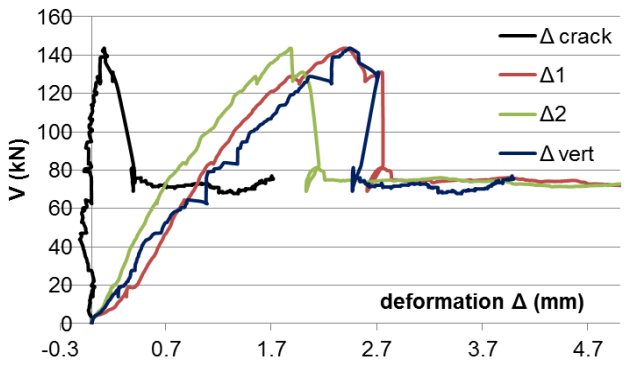

a) Push-off tests Load-Deformation curves for specimen HVFA-S-1 (with stirrups, no fibers)

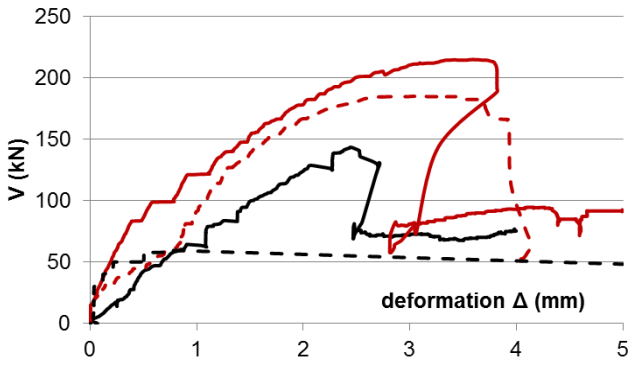

b) Push-off Load versus vertical deformation (Δ_{vert}) for different specimens

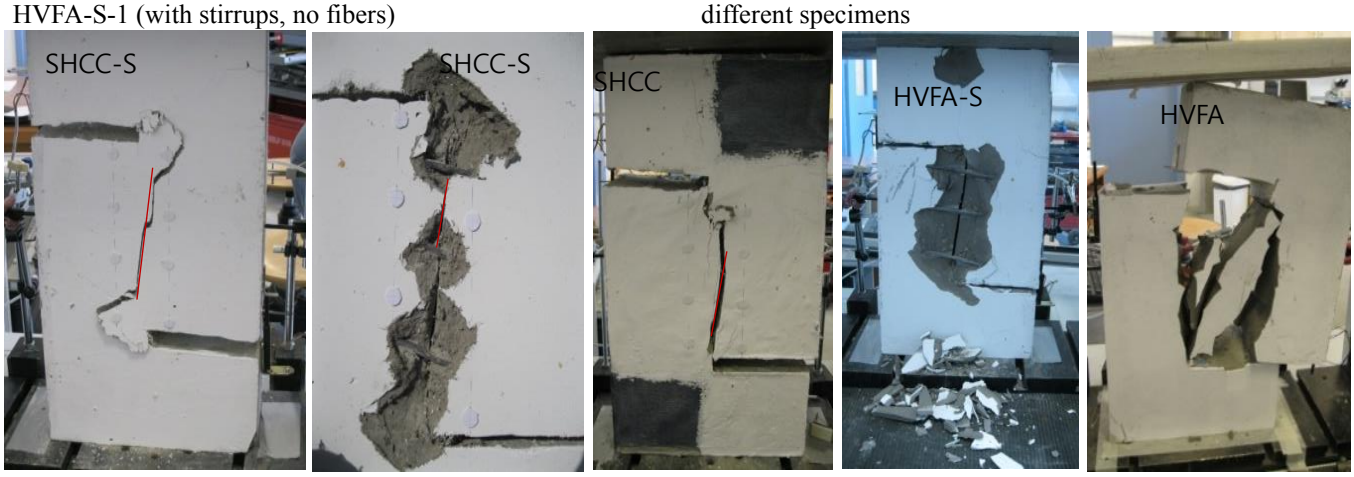

c) Push-off crack patterns for all specimens

Fig. 4 Push-off load-deformation and crack patterns

the shear plane and due to the absence of aggregates the friction on the shear plane was minimum and the full shear load was transferred through dowel action of the steel bars. Lateral deformation was initially concentrated at the main shear crack but as the vertical deformation increased the steel bars deformed as well, pushing off and delaminating the cover. The specimen with steel reinforcement (HVFA-S) started to delaminate rapidly with spalling of the cover after cracking at the shear plane. Spalling reached half of the width of the specimen (125 mm) and deformation of the steel reinforcement was visible over the entire deteriorated zone.

In the case of the fiber reinforced mix without stirrups multiple cracking was observed prior to crack localization and failure of the samples. The cracks formed in orientation inclined to the vertical shear plane, with evidence of compression crushing at the edges of the shear plane (Fig. 6). Failure of the fibers crossing the cracked planes was of a mixed type, ranging between rupture and pull-out. The width of the process zone (where cracks occurred) was approximately 40 mm but in no case was the composite delaminating laterally (i.e. the material maintained its integrity). The same type of crack development was evident in the fiber reinforced matrix with stirrups crossing the shear plane (Fig. 7). In these specimens though, the inclination of the cracks was greater than the inclination developed in the specimens without the steel reinforcement.

A small dislocation of the cracks occurred at the locations where the steel stirrups were crossing the cracks. The width of the process zone was in the order of 60 mm, without spalling of the fiber cementitious matrix. The tests in this case were terminated at the point where shear deformation was no longer possible – the vertical dislocation was enough to close the horizontal notches. Transverse reinforcement dowelled by 25 mm, a deformation that took place within the 60 mm process zone. The inclination angles of the cracks for the various specimens was, (a) θ=90º for HVFA, (b) θ=80.54º for HVFA-S, (c) θ=66.37º for SHCC, and (d) θ=83.38º for SHCC-S.

The experimental curves between the applied load and various measures of deformation of the push-off specimens (defined in Fig. 2. (d)) are plotted in the diagrams of Figure 4 (a). The crack opening Δ_{crack} ($\Delta_{crack}=\Delta_{6lvdt}+\Delta_{3lvdt}$) for the specimen with stirrups and no fibers (HVFA-S) shows a near to zero lateral expansion up to the maximum load. At maximum load the crack is created and after that, deformation accounts for the crack opening width. The small lateral expansion that develops prior to the maximum load is attributed to elastic deformations. At the beginning of the descending branch the load capacity diminishes from the peak value practically linearly with the increasing crack width, manifesting the loss of concrete contribution to shear resistance. The residual strength that continues at constant value to greater deformations, is the contribution of the steel

Fig. 5 Crack sequence on both sides of a specimen without fiber but with steel reinforcement crossing the shear plane (Specimen HVFA-S)

Fig. 6 Crack sequence on both sides of a specimen with fiber but without steel reinforcement crossing the shear plane (Specimen SHCC)

reinforcement to the shear capacity. The vertical deformation Δ_{vert} of the shear plane (between the crack faces) is in good agreement with the upper and lower recess deformations, Δ_1 and Δ_2 respectively (Fig. 2. (d)). Here the slope of the ascending branch shows that shear deformation increases with increasing shear resistance prior to crack localization, with vertical relative dislocations of the shear plane up to 2 mm (length of shear plane is 200 mm). After a crack is formed, shear capacity diminishes down to the contribution of the steel reinforcement crossing the shear plane.

Fig. 7 Crack sequence on both sides of a specimen with fiber and with steel reinforcement crossing the shear plane (Specimen SHCC-S)

Table 5 Push-off test results for all mixes

Specimen	f_c'	$f_{tsplitt}$	f_t	Max. Load	τ_{max}	$\tau_{max}/\sqrt{f_c'}$	τ_{max}/f_t
HVFA	50.37	1.62	-	54.49	2.49	0.35	1.31
HVFA-S	50.37	1.62	-	152.41	7.29	1.03	3.82
SHCC	48.98	6.4	2.65	186.82	9.17	1.31	3.33
SHCC-S	48.98	6.4	2.65	212.07	10.25	1.47	3.73

In Figure 4 (b) the diagrams of shear load versus normalized crack opening of one of the three specimens from each series are displayed for the push-off tests. The beam with the HVFA mix and without steel reinforcement showed abrupt failure at an average load of 54.5 kN. After the peak load that was accompanied by a strong noise the specimen was split in two pieces. Average shear stress attained by these specimens was in the order of 2.5 MPa, calculated as the total applied load divided by the cross sectional area under shear. Thus, addition of steel reinforcement (6 bars of 6 mm diameter) to the specimens in the absence of fibers increased the shear strength to 152.4 kN (average shear stress of 7.3 MPa), whereas the addition of fibers only by 2% by volume increased the shear strength to 186.8 kN (average shear stress of 9.17 MPa), that is, triple the value of the plain mix. Furthermore, the addition of fibers increased the shear deformation on the vertical axis of anti-symmetry of the specimen, and while the plain mix ruptures at a shear deformation of γ=0.5/200=0.25%, the mix with the fibers reaches a deformation of 3.5/200=1.75%. Shear stress sustained is significantly higher in the specimens with the fiber reinforced mixes, even though compressive strength of the SHCC mix is almost the same with that of the plain mix. This implies that shear strength is related mainly with the tensile stress-strain relationship of the mixes and not with the compressive strength. Stiffness of the specimens is greater in the case of the samples with stirrups, manifesting that steel reinforcement plays an important role in resisting shear even prior to crack initiation. In the case of the SHCC mix without the steel stirrups, cracking initiates at shear stresses close to 1/3 of the maximum shear stress of the samples and past that point stresses are transferred across the crack through the fibers, thereby developing a type of tension stiffening. At ultimate load of the plain SHCC specimen fibers start to rupture and the specimen collapses. All samples containing steel reinforcement after the ultimate load, exhibited a load drop down to an average shear stress of 4 MPa, where only stirrups continue to resist shear, and while this value remained constant in the case of the mix without the fibers, there was an increase in resistance in the case of the fiber reinforced matrix, relating dowel resistance of the stirrups to the tensile characteristics of the surrounding matrix.

Test results from all mixes are summarized in Table 5. Compressive strength is an average of three samples, as well as all averaged results obtained from the push-off tests. Average maximum shear stress τ_{max} is obtained by dividing the maximum load P, applied from the loading platen, divided by the area of the shear plane. Evidently, the average shear stresses developed in the HVFA specimens without steel reinforcement were higher than the direct tensile strength of the composite, while the introduction of steel reinforcement almost triples the shear capacity for the material without fibers. The introduction of fibers in the

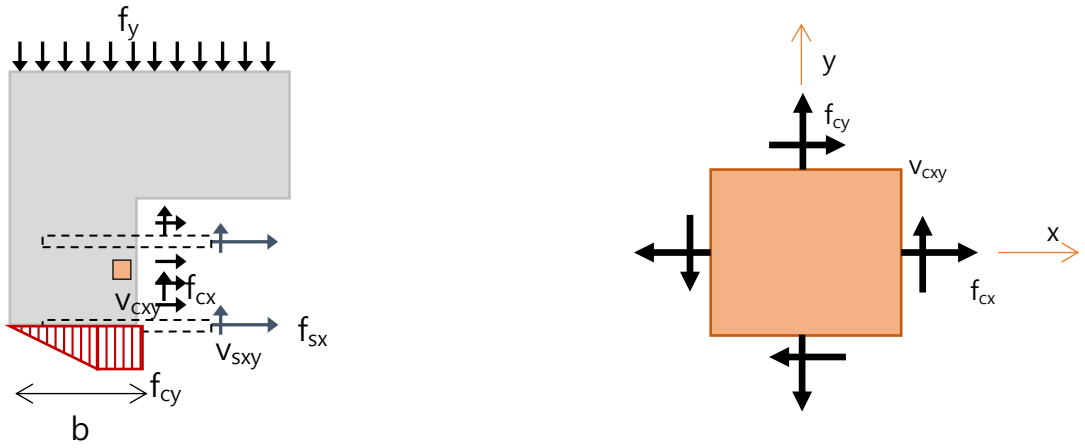

a) Push-off specimen free body diagram b) Infinitesimal element state of stress

Fig. 8 Infinitesimal element analysis

cementitious matrix triples the shear capacity of the cross section (from 55 MPa for HVFA to 186 MPa for SHCC). The use of PVA fibers results to shear strength in the order of 9.16 MPa, a value that is much greater than the tensile strength of the fiber reinforced composite. Adding fibers of 2% by volume results in a higher shear strength than those cases of plain concrete with steel reinforcement. Also, adding stirrups in the SHCC specimens is not as effective – increasing the shear capacity by only 10% over the unreinforced SHCC case.

5. Analysis of the results

5.1 Shear strength and dowel action mechanics

The average load capacity of the 100x200 mm cross section for the HVFA composite without steel reinforcement was 54.5 kN. The shear strength was τ_{ave} =2.5 MPa based on the push-off test, while tensile strength based on the splitting test was 1.62 MPa. The increase by 0.88 MPa in the case of the push-off test can be attributed to the relationship between tensile strength and shear strength at the onset of cracking. When steel reinforcement was crossing the critical cross section (HVFA-S) maximum load was increased to 152.4 kN but after the crack opened such that contact was lost between the opposite dislocating segments, the load dropped suddenly to an average of 75.74 kN, representing the dowel action of the stirrups.

In order to examine the influence of the materials' properties on the behavior of the specimens under direct push off, the problem is analyzed in terms of the stress state along the shear plane, by considering plane-stress transformation on an infinitesimal element of the free body of Fig. 8 (a) located at the midheight of the shear plane (Fig. 8 (b)). Forces acting on the free-body diagram are shown in Fig. 8 (a) by considering concrete as a new material with its own characteristics acting simultaneously with the reinforcement (Vecchio and Collins, 1986). The vertical stresses f_{cy} acting on the bottom side of the cut are assumed to have a triangular distribution being zero on the edge of the specimen, and increasing linearly over 2/3 of the breadth of the resisting section ($2b/3$) and the stress is considered constant on the remaining length of $b/3$. Normal stresses acting on the shear plane are those of the cementitious composite f_{cx} and of the steel reinforcement f_{sx}, while tangential components are v_{cxy} from concrete and v_{sxy} from the reinforcement. Equilibrium of forces on the x and y axis is given by Eq. 1 and 2, resulting in the stresses acting on an element of the material at the midheight of the shear plane as shown in Fig. 8 (b).

$$\int_A f_x dA = \int_{A_c} f_{cx} dA_c + \int_{A_s} f_{sx} dA_s = 0 \Rightarrow$$
$$\int_{A_c} f_{cx} dA_c = -\int_{A_s} f_{sx} dA_s \Rightarrow f_{cx} = -f_{sx} \cdot \rho_{sx} \quad (1)$$

$$\int_A f_y dA = \int_{A_c} v_{cxy} dA_c + \int_{A_s} v_{sxy} dA_s - \int_B f_{cy} dB$$
$$\rightarrow P = v_{cxy} A_c + v_{sxy} A_s - f_{cy} 2bd/3 \quad (2)$$

$$f_{cy} = -\frac{3P}{4b \cdot d}, \; v_{cxy} = \frac{P - v_{sxy} A_s}{A_c} \quad (3)$$

In the case of the HVFA and SHCC specimens with no steel reinforcement crossing the shear plane the stresses f_{cx}, f_{sx} and v_{sxy}, are set equal to zero for the HVFA, while in the case of the SHCC f_{cx} is taken equal to the splitting strength of the composites taken into consideration that the fibers acting on the cross section provide confinement to the composite. This results in shear stresses that are equal to the force acting on the specimen divided by the shear plane (b=125 mm, d=100 mm, A_c=20000 mm^2) minus the contribution of the vertical stresses f_{cy}. The value of the

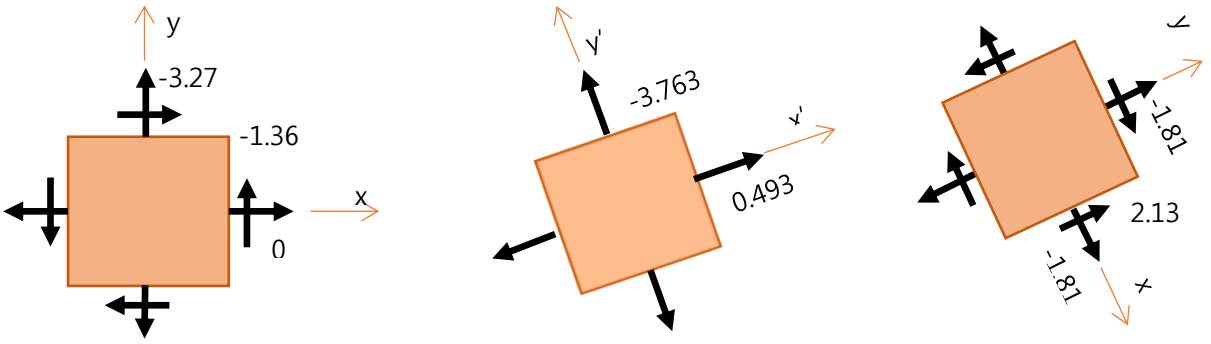

a) Element of HVFA b) Principal normal stresses c) maximum shear stresses

Fig. 9 HVFA stress analysis

shear stresses acting on the infinitesimal specimen was obtained from Equation 2 to be v_{cxy}=1.36 MPa and 4.67 MPa in the cases of the HVFA and SHCC respectively. These values are assumed to correspond to shear stresses v_{cxy} of the steel reinforced specimens HVFA-S and SHCC-S. With this approach the dowel action of the steel reinforcement is obtained from the difference of load resistance between otherwise identical reinforced and unreinforced specimens. The dowel action in the case of the HVFA-S specimen reaches values close to the yield strength of the stirrups (v_{sx}=288.6 MPa, by using Equation 2, setting v_{cxy}=1.36 MPa as obtained from the HVFA specimens) showing the great activation and deformation of the stirrups at the point of maximum load, while in the case of the SHCC-S, the dowel action only reached a stress of 74.4 MPa corresponding to the lower deformation rate due to the presence of the fibers. The orientation of the principal normal stresses θ_p (positive value rotates the x axis anticlockwise), the principal stresses σ_1 and σ_2, as well as the principal shear stress $\tau_{cxy,max}$ are calculated as per

$$\tan 2\theta_p = v_{cxy} / \left(0.5 \cdot \left(f_{cx} - f_{cy}\right)\right) \tag{4}$$

$$\sigma_x^{'} = 0.5 \cdot \left(f_{cx} + f_{cy}\right) + 0.5\left(f_{cx} - f_{cy}\right) \cdot \cos 2\theta_p + v_{cxy} \cdot \sin 2\theta_p = \sigma_1 \tag{5}$$

$$\sigma_y^{'} = 0.5 \cdot \left(f_{cx} + f_{cy}\right) - 0.5 \cdot \left(f_{cx} - f_{cy}\right) \cdot \cos 2\theta_p - v_{cxy} \cdot \sin 2\theta_p = \sigma_2 \tag{6}$$

$$\tau_{cxy,max} = \sqrt{v_{cxy}^2 + \left(0.5 \cdot \left(f_{cx} - f_{cy}\right)\right)^2} \tag{7}$$

Figure 9 plots the principal stresses and maximum shear stress in the case of an element of the HVFA specimen that has no steel reinforcement or fibers in the mix design. Table 6 gives the stress analysis results for the four different cases examined within this study. The horizontal stress on the cross section f_{cx} in the case of the SHCC is the internal confining stress effected by the fibers. The magnitude of this stress has been determined to be equal in magnitude and of opposite sign to the splitting cylinder tensile strength as per Georgiou and Pantazopoulou (2017b). In the case of the reinforced SHCC the horizontal stress is equal to the sum of the splitting tensile strength and the dowel action of the HVFA specimen. The maximum shear stresses τ_{xymax} and the angle of the shear plane θ_s are also listed in Table 6.

Table 6 Stress analysis of all specimens

Analysis parameters	HVFA	HVFA-S	SHCC	SHCC-S
ρ_{sx}	0	0.008482	0	0.008482
f_{sx} (MPa)	300	300	300	300
f_{cx} (MPa)	0.00	-2.54	-6.37	-8.91
f_{cy} (MPa)	-3.27	-9.14	-11.21	-12.72
P_{max} (kN)	54.49	152.41	186.82	212.07
v_{sxy} (MPa)	0.00	288.58	0.00	74.41
v_{cxy} (MPa)	1.36	1.36	4.67	4.67
θ_p (°)	19.90	11.22	31.31	33.91
σ_x=σ_1 (MPa)	0.49	-2.27	-3.53	-5.78
σ_y=σ_2 (MPa)	-3.76	-9.41	-14.05	-15.86
θ_s (°)	-25.1	-33.78	-13.69	-11.09
$\tau_{x'y'max}$ (MPa)	2.13	3.57	5.26	5.04

5.2 Design criteria for shear strength

The design for shear transfer proposed in the ACI Building Code, (ACI 318M-14, 2015), uses the "shear-friction" hypothesis proposed by (Birkeland and Birkeland, 1966) and (Mast, 1968). This is a simplified approach where shear strength v_u is calculated based on Eq. 8 for concrete with shear transfer strength up to 0.2f_c or 5.5 MPa (whichever is less) with a friction coefficient μ=1.4. Mattock and Hawkins 1972 based on experimental data propose an alternative approach, for sections with active confinements between 1.4 MPa and 0.3f_c as per Eq. 9.

$$v_u = \frac{A_s \cdot f_y}{b \cdot d} \cdot \mu \tag{8}$$

$$v_u = 1.4 + 0.8\left(\frac{A_s \cdot f_y}{b \cdot d} + \sigma_x\right) \tag{9}$$

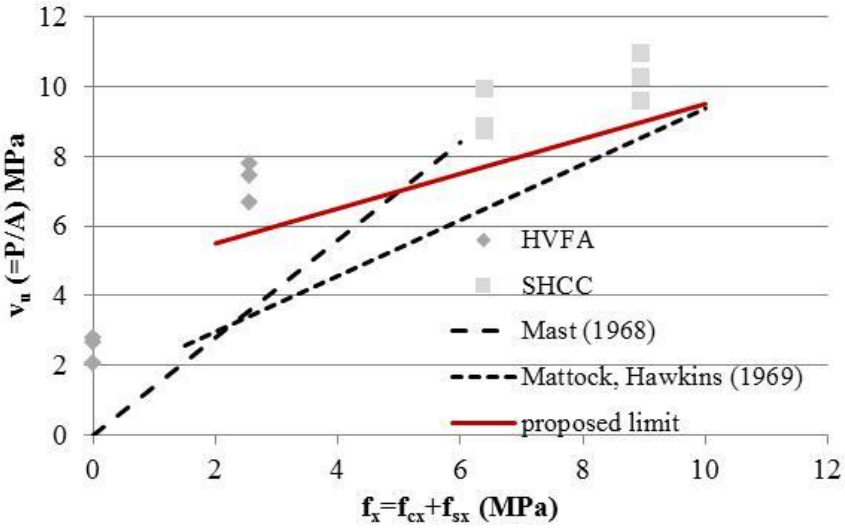

Fig. 10 Shear strength vs active confinement (test results and comparison with proposed limits)

Where A_s is the area of the stirrups crossing the shear plane, f_y is the yield strength of the stirrups, b, d are the dimensions of the shear plane, μ is the friction coefficient and σ_x is active lateral confinement. The experimental results of the shear strength vs the confinement provided are plotted in Fig. 10 and are compared to Eq. 8 and 9. The lateral confinement of the experimental data is found by the infinitesimal element analysis provided in Table 6. The results indicate that Eq. 8 and 9 are not able to provide the actual shear strength of fiber reinforced cementitious composites as they have been calibrated based on normal concrete. The experimental results are used to calibrate a new proposed limit equation that takes into consideration the active confinement imparted by the fibers, by using the splitting tensile strength (f_{tsplit}) of the SHCC as per Eq. 10.

$$v_u = 4.5 + 0.5\left(\frac{A_s \cdot f_y}{b \cdot d} + f_{tsplit}\right) \quad (10)$$

5. Conclusions

In this paper the behavior of SHCC under direct shear was experimentally and analytically investigated. A series of identical push-off tests were conducted on specimens of the matrix without fibers and on the SHCC samples, in order to obtain the contribution of the fibers to shear. Additionally the same tests were conducted on specimens that contained steel reinforcement crossing the shear plane in order to investigate the combined action of conventional stirrups and fibers and to estimate the contribution of fibers to shear strength of SHCC. SHCC is a new type of sustainable cementitious mix design consisting of 55% of cement replacement with Fly Ash (Class F), with no coarse aggregate in the mix design and a low water-binder content. The shear capacity of this ductile cementitious composite differs from that of normal concrete wherein aggregate interlock is an important contributor to shear strength. The research showed that the composite was improved due to the use of short discontinuous Polyvinyl Alcohol (PVA) fibers at 2% by volume of the total mix. The materials' improved performance under tension and compression is also evident in enhanced shear strength and ductility under shear dislocation. The use of fibers multiplies the shear strength by three-fold over that of the plain matrix, while it is also by 30% greater than that provided by the use of steel stirrups alone. The results showed a correlation of the push off shear stress to the splitting tensile strength of the cementitious composite materials used for the specimens but not to the direct tensile strength. A new equation is proposed based on the experimental results to determine the shear strength of SHCC for design purposes.

References

ACI 318M-14 (2015), Building Code Requirements for Reinforced Concrete, American Concrete Institute, Michigan, USA.

Archontas, N.D. and Pantazopoulou, S.J. (2015), "Microstructural behavior and mechanics of nano-modified cementitious materials", *Adv. Concrete Construct.*, **3**(1), 15-37. https://doi.org/10.12989/acc.2015.3.1.015.

ASTM C496 (2006), "Standard test method for splitting tensile strength of cylindrical concrete specimens", ASTM International, Pennsylvania, USA.

ASTM C618 (2008), "Standard Specification for Coal Fly Ash and Raw or Calcined Natural Pozzolan for Use", ASTM International, Pennsylvania, USA.

Birkeland, P. W. and Birkeland, H. W. (1966), "Connections in Precast Concrete Construction", *J. American Concrete Inst.*, **63**(6), 345-368.

Buyukozturk, O., Bakhoum, M and Beattie, S. (1990), "Shear behavior of joints in precast concrete segmental bridges", *J. Struct. Eng.*, **116**(12), 3380-3401. https://doi.org/10.1061/(ASCE)0733-9445(1990)116:12(3380).

Campione, G., La Mendola, L and Papia, M. (2006), "Shear strength of steel fiber reinforced concrete beams with stirrups", *Struct. Eng. Mech.*, **24**(1), https://doi.org/10.12989/sem.2006.24.1.107.

Chang-Geun, C., Gee-Joo, H. and Yun-Yong, K. (2008),

"Nonlinear model of reinforced concrete frames retrofitted by infilled HPFRCC walls", *Struct. Eng. Mech.*, **30**(2), 211-223. https://doi.org/10.12989/sem.2008.30.2.211.

EN 12350-8:2010 (2010), "Testing fresh concrete Part 8: Self - compacting concrete - Slump- flow test", European Committee for Standardization.

EN 206:2013 (2013), "Concrete - Specification, performance, production and conformity", European Committee for Standardization.

Georgiou, A.V. and Pantazopoulou, S.J. (2016a), "Mechanical properties of fiber reinforced cementitious composites with high amounts of fly ash as cement replacement", *ICCS16 Second International Conference on Concrete Sustainability*, Madrid, Spain.

Georgiou, A. V and Pantazopoulou, S. J. (2016b), "Effect of fiber length and surface characteristics on the mechanical properties of cementitious composites", *Construct. Build. Mater.*, **125**(10), 1216-1228. https://doi.org/10.1016/j.conbuildmat.2016.09.009.

Georgiou, A. V and Pantazopoulou, S. J. (2016c), "Use of waste fly ash from power plants for use in cementitious composites for structural elements", *4th International Conference on Sustainable Solid Waste Management*, Limasol, Cyprus. June.

Georgiou, A.V. and Pantazopoulou, S.J. (2017), "Behavior of strain hardening cementitious composites in flexure/shear", *J. Mater. Civil Eng.*, **29**(10), 4017192. http://doi.org/10.1061/(ASCE)MT.1943-5533.0002041

Georgiou, A.V. and Pantazopoulou, S.J. (2018), "Experimental investigation on the confining effect of fibers in SHFRCC", *Compos. Struct.*, **102**, 29-37. https://doi.org/10.1016/j.compstruct.2017.09.110.

Kang, S., Tan, K., Zhou, X.H., Yang, B. (2017), "Experimental investigation on shear strength of engineered cementitious composites", *Eng. Struct.*, **143**, 141-151. https://doi.org/10.1016/j.engstruct.2017.04.019.

Li, V.C., Wu, C., Wang, S., Ogawa, A and Saito, T. (2003), "Interface tailoring for strain-hardening Polyvinyl Alcohol-Engineered Cementitious Composite (PVA-ECC)", *ACI Mater. J.*, **99**(5), 463-472.

Mast, R.F. (1968), "Auxiliary reinforcement in concrete connections", *Proceedings ASCE*, **94**(ST6), 1485-1504.

Mattock, A.H and Hawkins, N.M. (1972), "Shear transfer in reinforced concrete-recent research", *PCI J.*, **77**(2), 55-79.

Naaman, A.E. and Reinhardt, H. (2006), "Proposed classification of HPFRC composites based on their tensile response", *Mater. Struct.*, **39**(5), 547-555. https://doi.org/10.1617/s11527-006-9103-2.

Orod, Z., Hamid Reza, K. (2016), "Experimental investigation on self-compacting concrete reinforced with steel fibers", *Struct. Eng. Mech.*, **59**(1), 133-151. https://doi.org/10.12989/sem.2016.59.1.133.

Parra-Montesinos, G.J. (2005), "High-performance fiber-reinforced cement composites: An alternative for seismic design of structures", *ACI Struct. J.*, **102**(5), 668-675.

Qissab, M. A. and Salman, M. M. (2018), "Shear strength of non-prismatic steel fiber reinforced concrete beams without stirrups", *Struct. Eng. Mech.*, **67**(4), 347-358. https://doi.org/10.12989/sem.2018.67.4.347.

Toshiyuki, K., Kabele, P., Fukuyama, H., Uchida, Y., Suwada, H and Slowik, V. (2013), *Strain Hardening Cement Composites: Structural Design and Performance*, Springer, Netherlands. http://doi.org/10.1007/978-94-007-4836-1

Valle, M and Buyukozturk, O. (1993), "Behavior of fiber reinforced high-strength concrete under direct shear", *ACI Mater. J.*, **90**(2), 122-133.

Vecchio, F.J and Collins, M.P. (1986), "The modified compression field theory for reinforced concrete elements subjected to shear", *ACI Struct. J.*, **83**(2), 219-231.

Wang, S. and Li, V.C. (2006), "Polyvinil alcohol fiber reinforced engineered cementitious composites: material design and performances", *Proceedings of International workshop on HPFRCC in Structural Applications*, Honolulu, Hawaii, USA.

Zhao, P.Z., Kanf, S.B., Yang, B. (2017), "Shear strength of engineered cementitious composites under Push-Off Loads", *Proceedings of 6th International Workshop on Performance, Protection and Strengthening of Structures under Extreme Loading*, Guangzhou (Canton), China, December.

CC